Tunable Active Microwave Bandpass Filters

Using Three-terminal MESFET Varactors

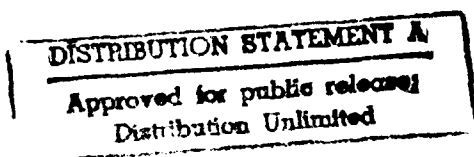Jenshan Lin and Tatsuo Itoh
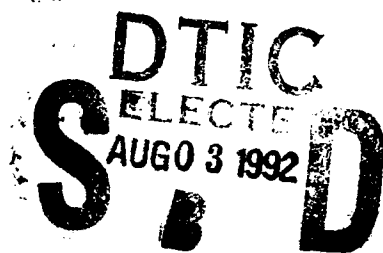
DTIC
ELECTE
AUG 0 3 1992
S D

January 27, 1991

University of California, Los Angeles

School of Engineering and Applied Science

92-20876

92 7 31 161

REPORT DOCUMENTATION PAGE

1a. REPORT SECURITY CLASSIFICATION		1b. RESTRICTIVE MARKINGS			
Unclassified					
2a. SECURITY CLASSIFICATION AUTHORITY		3. DISTRIBUTION/AVAILABILITY OF REPORT			
2b. DECLASSIFICATION / DOWNGRADING SCHEDULE		Approved for public release; distribution unlimited.			
4. PERFORMING ORGANIZATION REPORT NUMBER(S)		5. MONITORING ORGANIZATION REPORT NUMBER(S)			
UCLA Report No. ENG-92-29		ARO 25045.67-EL			
6a. NAME OF PERFORMING ORGANIZATION	6b. OFFICE SYMBOL (If applicable)	7a. NAME OF MONITORING ORGANIZATION			
University of Texas / UCLA		U. S. Army Research Office			
6c. ADDRESS (City, State, and ZIP Code)		7b. ADDRESS (City, State, and ZIP Code)			
405 Hilgard Avenue Los Angeles, CA 90024		P. O. Box 12211 Research Triangle Park, NC 27709-2211			
8a. NAME OF FUNDING/SPONSORING ORGANIZATION	8b. OFFICE SYMBOL (If applicable)	9. PROCUREMENT INSTRUMENT IDENTIFICATION NUMBER			
U. S. Army Research Office		DAAL03-88-K-0005			
8c. ADDRESS (City, State, and ZIP Code)		10. SOURCE OF FUNDING NUMBERS			
P. O. Box 12211 Research Triangle Park, NC 27709-2211		PROGRAM ELEMENT NO.	PROJECT NO.	TASK NO.	WORK UNIT ACCESSION NO.

11. TITLE (Include Security Classification)

Tunable Active Microwave Bandpass Filters Using Three-terminal MESFET Varactors

12. PERSONAL AUTHOR(S)   Jenshan Lin and Tatsuo Itoh

13a. TYPE OF REPORT	13b. TIME COVERED	14. DATE OF REPORT (Year, Month, Day)	15. PAGE COUNT
Technical	FROM _____ TO _____	1992, January 27	57

16. SUPPLEMENTARY NOTATION The view, opinions and/or findings contained in this report are those of the author(s) and should not be construed as an official Department of the Army position, policy, or decision, unless so designated by other documentation.

17. COSATI CODES			18. SUBJECT TERMS (Continue on reverse if necessary and identify by block number)
FIELD	GROUP	SUB-GROUP	Microwave Bandpass Filters, Tunable Active Filters
			Three-terminal MESFET Varactors

19. ABSTRACT (Continue on reverse if necessary and identify by block number)

Two types of tunable active bandpass filter working at X-band are presented. Both circuits employ the concept of three-terminal MESFET varactor. The first circuit uses two MESFETs of which one is used to generate a negative resistance and the other is used to generate a variable reactance. The second circuit uses only one MESFET which has both functions of those two MESFETs in the first circuit. The achievement of using one MESFET to replace two MESFETs with different functions provides a significant advantage. It reduces the number of solid-state elements needed in the active circuits and thus simplifies the fabrication of the circuits.

20. DISTRIBUTION/AVAILABILITY OF ABSTRACT		21. ABSTRACT SECURITY CLASSIFICATION
☐ UNCLASSIFIED/UNLIMITED ☐ SAME AS RPT. ☐ DTIC USERS		Unclassified
22a. NAME OF RESPONSIBLE INDIVIDUAL	22b. TELEPHONE (Include Area Code)	22c. OFFICE SYMBOL
Tatsuo Itoh	(310)206-4820	

ABSTRACT

Two types of tunable active bandpass filter working at X-band are presented. Both circuits employ the concept of three-terminal MESFET varactor. The first circuit uses two MESFETs of which one is used to generate a negative resistance and the other is used to generate a variable reactance. The second circuit uses only one MESFET which has both functions of those two MESFETs in the first circuit. The achievement of using one MESFET to replace two MESFETs with different functions provides a significant advantage. It reduces the number of solid-state elements needed in the active circuits and thus simplifies the fabrication of the circuits.

DTIC QUALITY INSPECTED 5

Accession For		
NTIS GRA&I		☑
DTIC TAB		☐
Unannounced		☐
Justification		
By		
Distribution/		
Availability Codes		
Dist	Avail and/or Special	
A-1		

Table of Contents

List of Figures

List of Tables

Chapter 1
Introduction

Recently, a microstrip-line circuit of tunable active bandpass filter working at X-band has been made. A half-wavelength microsrtrip resonant tank is used as the core of this type of circuit to create a narrow passband. Because the loss of resonant tank including conduction loss, substrate loss, and radiation loss is large, a coupled negative resistance method is introduced by Chang to compensate the loss[1]. This makes the circuit active.

Chang divided the half-wavelength tank into two quarter-wavelength sections and connected them by a varactor diode(Fig. 1.1). By changing the bias voltage of the varactor diode, the center frequency of passband can be tuned[1]. Yamamoto connected the two quarter-wavelength sections through the gate and the source of a GaAs MESFET. This MESFET, which is the same type of device as the element used to create the negative resistance, works as a varactor. By changing the bias voltage the center frequency of passband can also be tuned[2].

In addition to voltage-control tuning, MESFETs can be used as an optically controlled varactor. Yamamoto carried out this concept by removing the package cover of the MESFET so that the gate-to-source depletion region can be illuminated by a semiconductor laser diode[3]. The laser light generates some electron-hole pairs inside the depletion region and thus change the gate-to-source capacitance.

The varactors Chang and Yamamoto used are both two-terminal varactors. However, the MESFET that Yamamoto used can also be used as a three-terminal varactor by using all three variable parameters C_{gs}, C_{gd} and C_{ds}. In Chapter 2, this concept is discussed and the behavior of these variable reactances is studied.

Based on the concept of three-terminal MESFET varactor, a tunable active bandpass filter using two MESFETs was made. One MESFET is biased in the active mode to

generate a negative resistance. The other is biased in the reactive mode and acts as a three-terminal varactor to changes the effective electrical length of the half-wavelength resonant tank by the T-junction method. The concept, the design and the measurement result of this circuit are given in Chapter 3.

The most significant advantage of using the three-terminal MESFET varactor is that the functions of the negative resistance MESFET and the three-terminal MESFET varactor can be combined together into one MESFET. That is, the MESFET can play both roles at the same time. This means we can replace those two MESFETs needed in the circuit described above with only one MESFET. Based on this concept, a tunable active bandpass filter using only one MESFET is made. In Chapter 4, the design of this circuit and the measurement result are discussed.

Chapter 2
Three-terminal MESFET Varactor

2.1 Two-terminal Varactor

The term "varactor" comes from the words *variable reactor*, which means a device with a variable reactance. A PN junction diode is usually used as a varactor diode. By changing the reverse-bias voltage, the width of the depletion region is changed and thus the capacitance is changed(Fig. 2.1).
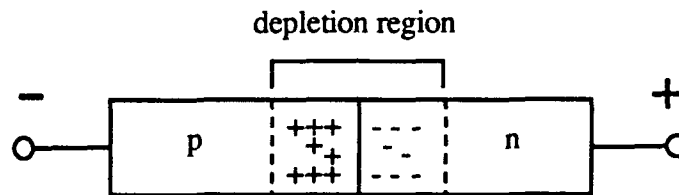
depletion region

Fig. 2.1   PN junction of a varactor diode

The MESFET can also be a two-terminal varactor by using its depletion region. A negative voltage is applied on the gate to create a depletion region. The drain is either connected to the source or is open-circuited(Fig. 2.2). The gate-to-source capacitance is a function of the bias voltage or the intensity of incident light(Fig. 2.3). If the gate-to-source capacitance is controlled by the incident light, then it is an optically controlled varactor[3].
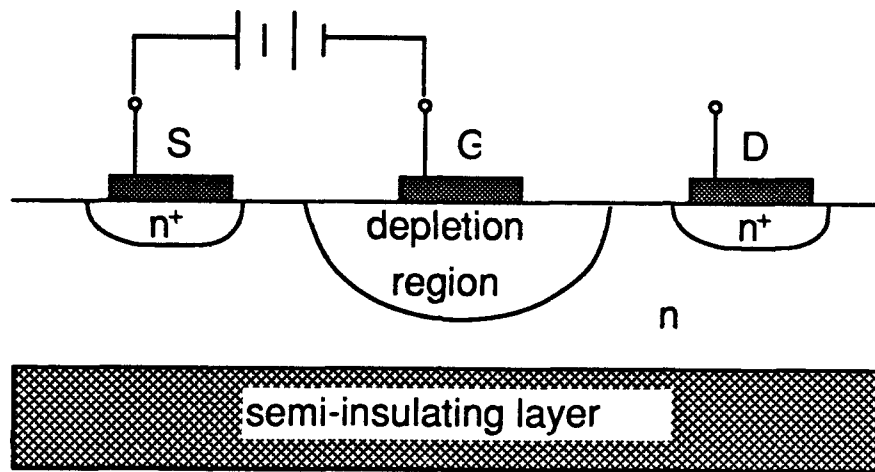
(a) The drain is open-circuited
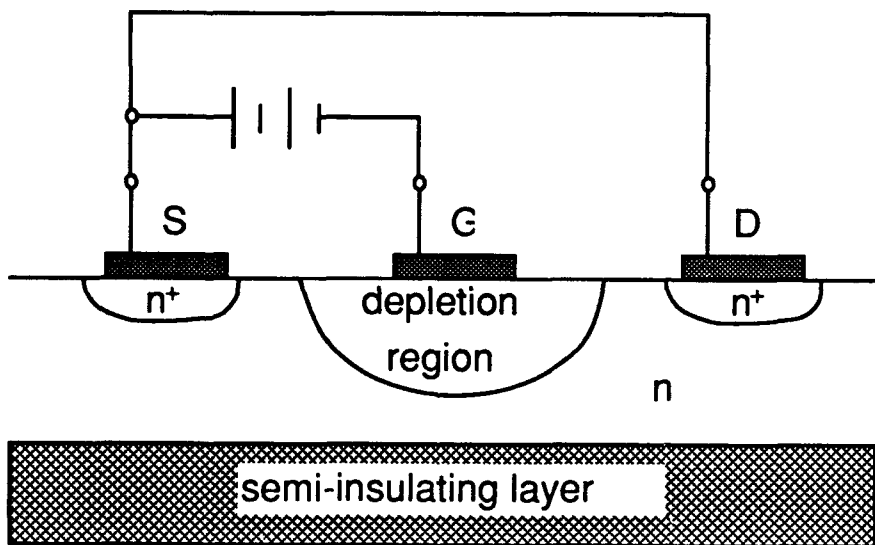
(b) The drain is connected to the source

Fig. 2.2 Using the MESFET as a two-terminal varactor

4
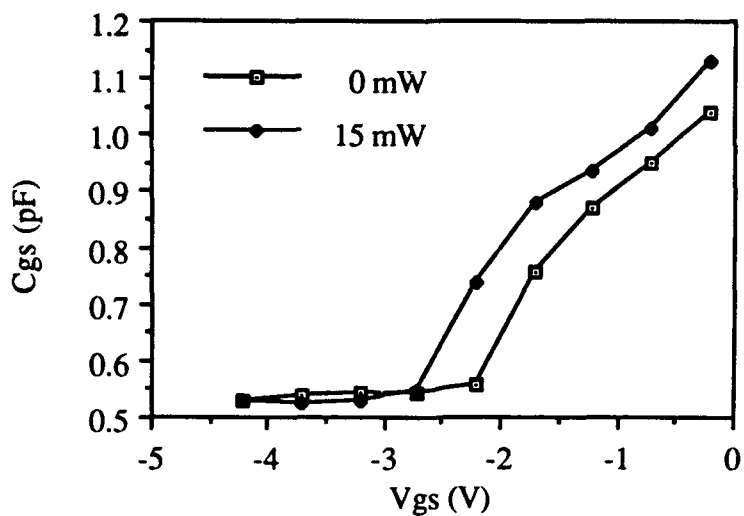
(a) C_{gs} of the MESFET as a function of V_{gs} at two different levels of light

illumination: $P_L = 0$ mW and $P_L = 15$ mW (P_L is the output power of

a semiconductor laser diode, Sharp LT021MC0)
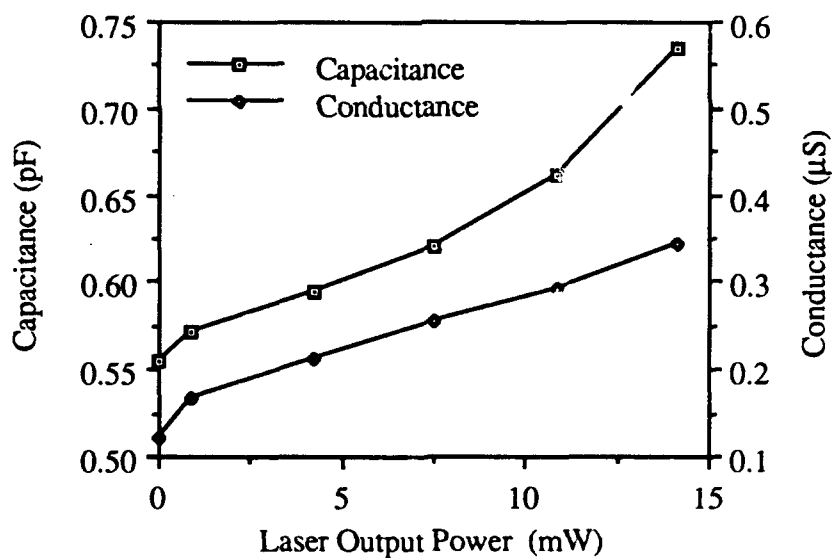
(b) C_{gs} and G_{gs} as a function of the output power from a semiconductor laser diode

(Sharp LT021MC0). Bias voltage (V_{gs}) = -2.21V[4]

Fig. 2.3   Gate-to-source capacitance of the MESFET

5

With the aid of such two-terminal varactors to change the effective electrical length of the resonant tank(Fig. 2.4), the center frequency of the passband of an X-band active filter can be tuned[1][2].
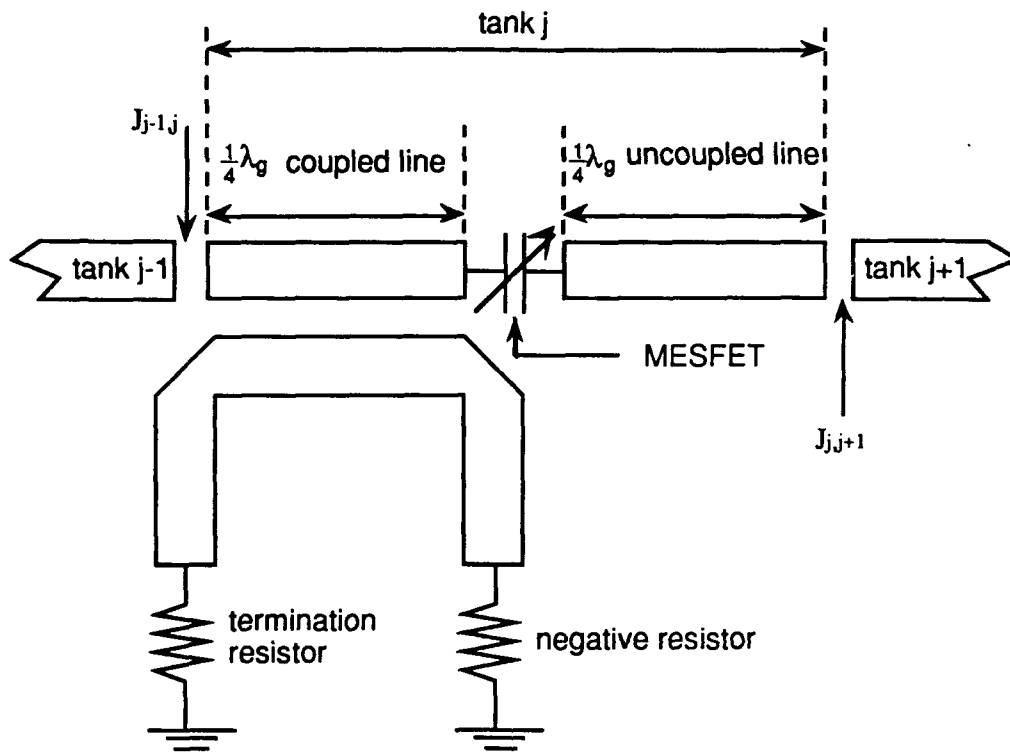
Fig. 2.4 Resonant tank of an X-band tunable active bandpass filter

2.2 Using MESFET As Three-terminal Varactor

Eventually, the MESFET is a three-terminal device designed for amplifying signal. Beside this, it is used as a varactor as described in the previous section. However, the MESFET is treated as a two-terminal device in this case. In the configuration of Fig. 2.2(a), only gate-to-source capacitance(C_{gs}) is used. In the configuration of Fig. 2.3(b), both gate-to-source capacitance(C_{gs}) and the gate-to-drain capacitance(C_{gd}) are used and parallel-connected.

Beside C_{gs} and C_{gd}, there is another capacitance C_{ds} exists between drain and source. A reactive MESFET model based on these three parameters is shown in Fig. 2.5. The effect of resistance is neglected here. Therefore, if we use the MESFET as a three-terminal device in a one-port circuit, these three parameters as well as the transmission-line parameters are combined together to create a reactance X_{in} at the input port of this circuit(Fig. 2.6). Since C_{gs}, C_{gd} and C_{ds} are all variable, the reactance X_{in} is also variable. Its value can be changed by the DC bias of MESFET or by the optically controlled method described in section 2.1. When this reactance X_{in} is applied to the tank circuit, the resonant length of tank can be changed by changing X_{in}, and thus the resonant frequency is changed.
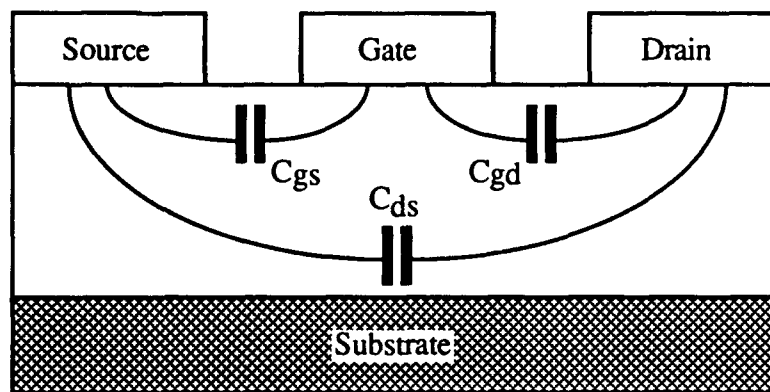
Fig. 2.5 Reactive MESFET model
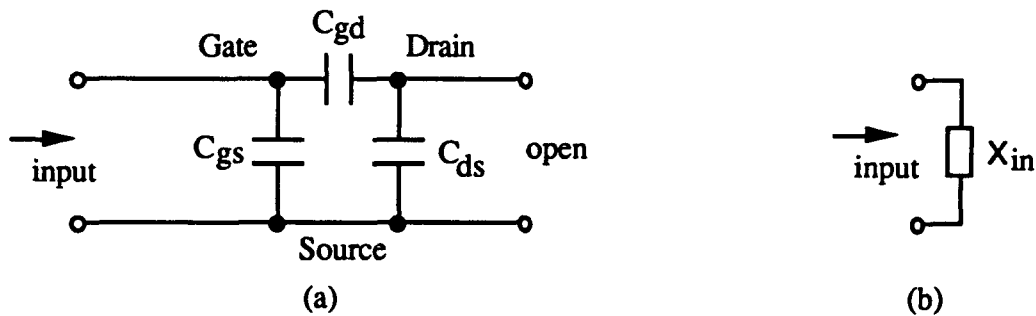
Fig. 2.6   (a) Using the reactive MESFET in one-port circuit

(b) Equivalent circuit of (a)

In the three-terminal configuration, most GaAs MESFET models consider C_{gs} and C_{gd} as voltage-dependent capacitances and C_{ds} as voltage-independent capacitance. C_{gs} and C_{gd} are thought of as capacitances of equivalent Schottky barrier diodes between the gate and source and gate and drain, respectively[5]. For a negative gate-source voltage and a small drain-source voltage, each diode is reverse biased about the same amount and the capacitances C_{gs} and C_{gd} are about equal. As the drain-source voltage is increased, the depletion region on the drain side extends and C_{gd} becomes smaller than C_{gs}. When the drain-source voltage is increased beyond the point of current saturation, C_{gd} is much smaller than C_{gs} which becomes dominant[6]. In such models capacitances of Schottky barrier diodes are considered and the capacitance change due to the gate voltage can be explained by the space charge model. The dependence is shown in Fig. 2.3(a).

A better capacitance model which considers both the Schottky capacitances and the fringing sidewall capacitances was proposed by Takada et al[7]. However, this model is limited by small drain voltages. At small drain voltages, the charge accumulation on the

8

drain-side edge and the source-side edge of depletion region is negligibly small. In this model, the variable capacitances considered are still C_{gs} and C_{gd}.

The dependence on the drain voltage is more complicated. The C-V dependence between drain and source terminals are measured at 1 MHz on HP 4280A C-V meter. At different gate voltages, the V_{ds}-dependence of this capacitance is plotted in Fig. 2.7. When the gate voltage is larger than the pinch-off voltage, the channel is open and the conductance becomes very large. This results in a large measurement error. The pinch-off voltage given by the manufacturer is -1.5V, which is in agreement with the measurement result. When the channel is pinched-off the C-V curves show the tendency of the increased capacitance as V_{ds} is increased. This voltage dependence is in agreement with the data calculated by Willing et al[8]. However, this voltage-dependence cannot be explained by C_{gs} and C_{gd} since both capacitances decrease as V_{ds} increases.

The charge accumulation in the active channel plays an important role here. When the drain-source current is saturated, the active channel capacitance which comes from the charge accumulation effect increases monotonically as V_{ds} increases. This phenomenon was first reported by Engelmann and Liechti[9] and was elaborated by Willing et al[8]. This nonlinear effect predicts that the capacitance C_{ds} dependents on V_{ds} when the drain-source current is saturated. When the drain voltage increases, the amount of charge accumulation increases and the capacitance between drain and source terminals increases.

Based on the theory presented above, two kinds of tunable active bandpass filter are made. Both circuits use the MESFET as a three-terminal device. The design and the fabrication are described in the following two chapters. The circuit performance is measured and the result is explained by the reactive MESFET model presented in this chapter.
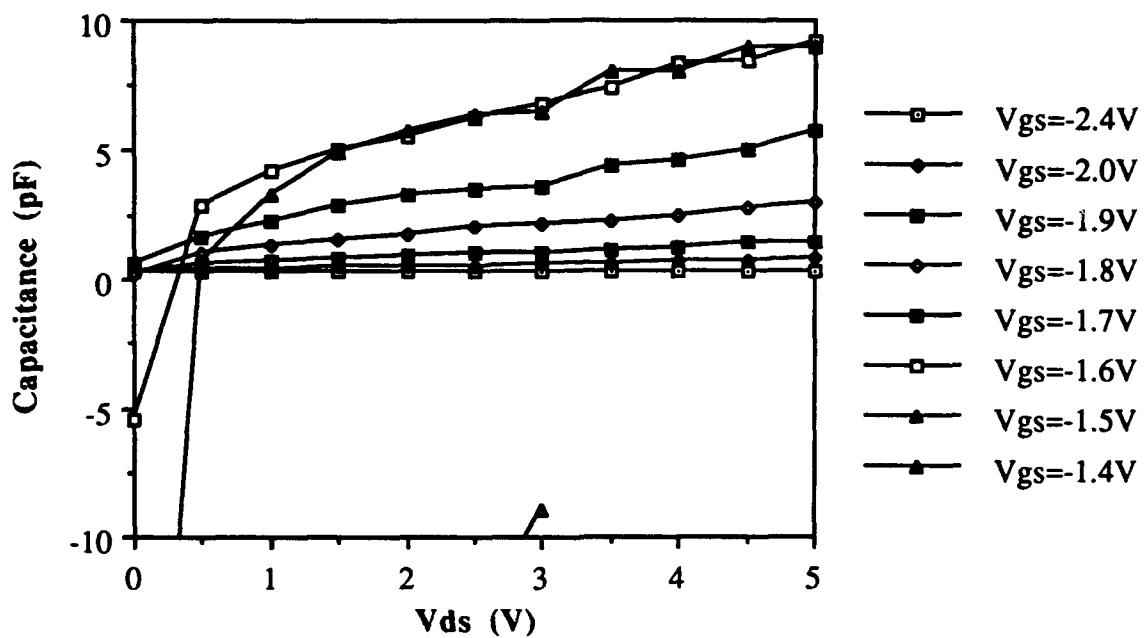
Fig. 2.7   C-V measurement of the MESFET between drain and source terminals

Chapter 3
Tunable Active Bandpass Filter Using Two MESFETs

In this chapter, a tunable active bandpass filter using two MESFETs is presented. One MESFET is used to generate a negative resistance which compensates the loss in the resonant tank. The other MESFET is used as a three-terminal varactor described in chapter two to tune the center frequency of the passband. To change the electrical length of resonant tank, the T-junction method is adopted so that the change of reactance in the reactive MESFET is coupled into the resonant tank. Both the voltage-control tuning and the optical-control tuning are measured and explained by the reactive MESFET model in Chapter two.

3.1 Circuit Design, Simulation and Fabrication

The basic structure of this circuit is a passive bandpass filter with an end-coupled half-wavelength resonator as shown in Fig. 3.1. The system impedance is designed to be 82 Ohm at 10 GHz and is tapered to be 50 Ohm to match the input impedance and the output impedance. To compensate the loss of the resonator, a negative resistance is added to the resonant tank through the coupled-line method(Fig. 3.2). The device which creates the negative resistance is NE72084B GaAs MESFET. The substrate is PTFE with dielectric constant of 2.55 and thickness of 30 mil.
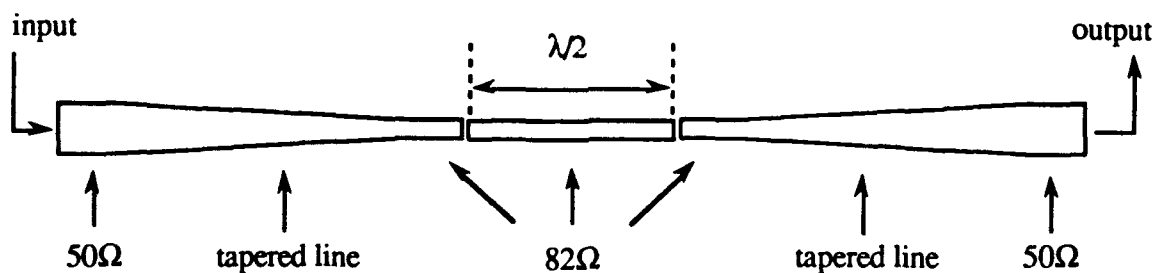
Fig. 3.1 Passive bandpass filter
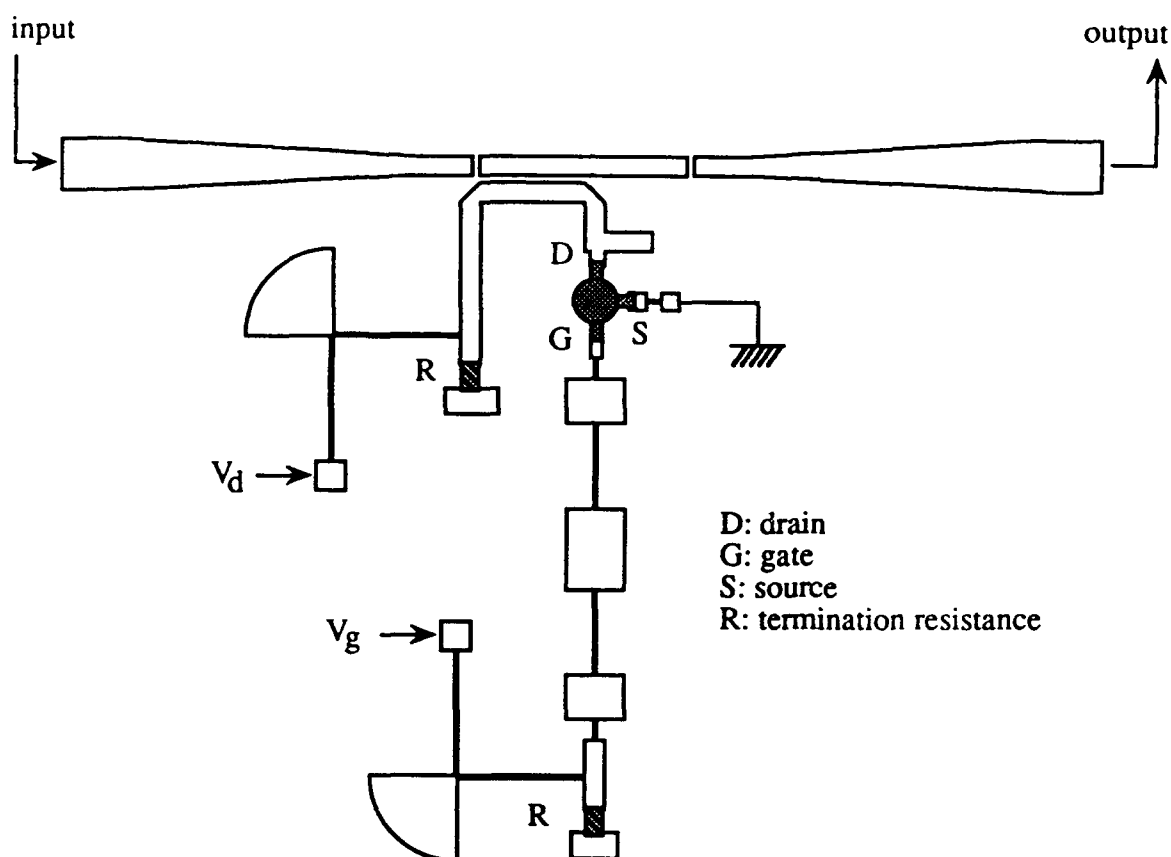
Fig. 3.2 Active bandpass filter with negative resistance

In order to make the filter in Fig. 3.2 tunable, the effective electrical length of the resonant tank needs to be changed by an appropriate mechanism. A reactance-tuning circuit is designed for this purpose. The idea of this circuit shown in Fig. 3.3 comes from Fig. 2.6. The MESFET is used as a three-terminal device in this one-port circuit. To be reactive, the transmission line connected to the drain terminal is open at the other end. The transmission line connected to the source terminal is shorted at the other end for the same reason. The reason why it is shorted but not opened is to satisfy the DC bias model in which the source terminal is connected to the ground. In case where the MESFET is not

12

operated in the active mode and the effect of conductances is negligible, the circuit generates a reactance at the input port. That is, the input impedance of this circuit is purely imaginary.
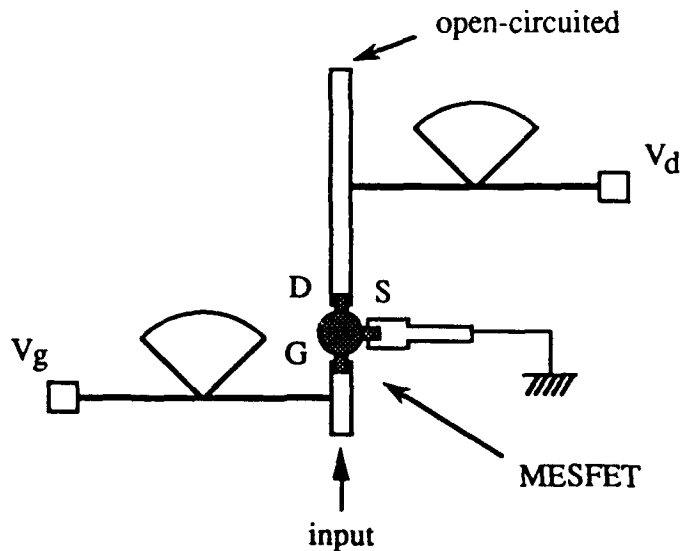
Fig.3.3 Reactance-tuning circuit using the MESFET

The input impedance Z_i of this reactance-tuning circuit is simulated by the Touchstone™ simulator. The simulation result is shown in Fig. 3.4. The S-parameter set of the MESFET used in simulation is for the bias condition of $V_{ds}=3V$ and $I_{ds}=10mA$. Since the MESFET is in the active mode under this bias condition, the real part of Z_i has negative value. The transmission lines connected to the MESFET are intended to reduce the magnitude of $Re[Z_i]$ between 9.5 GHz and 10.5 GHz. This is the expected frequency-tuning range. When the bias condition of the MESFET is changed, the curve of $IM[Z_i]$ is shifted left or right because the effective electrical length inside the MESFET is changed. Therefore, a reactance-tuning circuit is made.

13
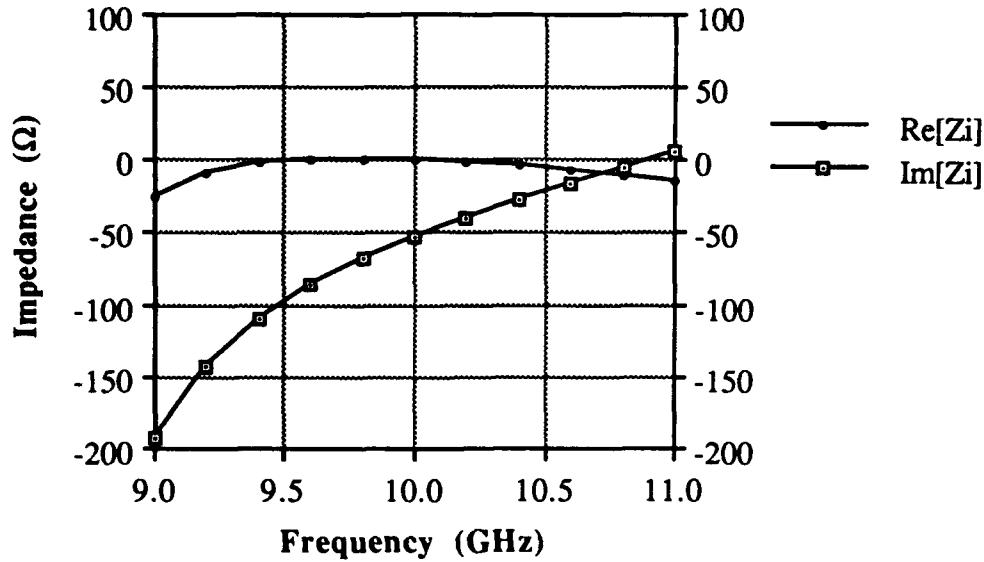
Fig. 3.4   Simulation result of the reactance-tuning circuit

The reactance-tuning circuit is then attached to the active filter circuit in Fig. 3.2 by T-junction method. To prevent destroying the resonance in the tank, the reactance cannot be added anywhere except at the center portion. However, the frequency tuning range is very small if this imported reactance is added right at the center point. This is because the electric field at this point is zero under resonance and cannot excite a dominant mode into the reactance-tuning circuit. Therefore, a position at which the left side of the imported transmission line and the center line of resonant tank coincide is determined. The frequency tuning ranges of these two positions are compared in Fig. 3.5. Under the same bias condition, the tuning range is 50 MHz for the configuration (a) while it is 150 MHz for the configuration (b).

14
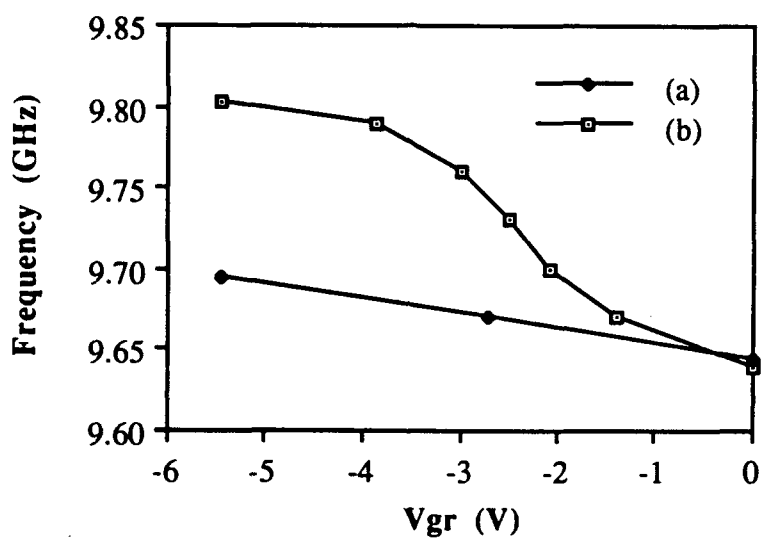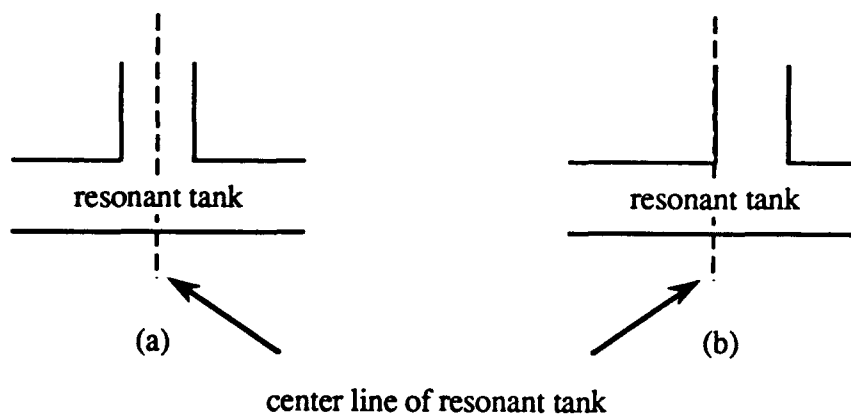
Fig. 3.5 Comparison of the frequency tuning ranges for

two different cases

V_{gr} : gate voltage of the reactive MESFET

V_{dr} : drain voltage of the reactive MESFET

V_{gn} : gate voltage of the MESFET as negative resistance

V_{dn} : drain voltage of the MESFET as negative resistance

Bias condition : V_{gn} = - 0.98V, V_{dn} = 3.29V, V_{dr} = 0V

The final circuit pattern of the tunable active bandpass filter using two MESFETs is drawn in Fig. 3.6. Details of the circuit parameters are listed in Appendix A. The simulation result of the circuit performance at fixed bias condition is shown in Fig. 3.7. This circuit pattern is then fabricated on the RT/duroid® ULTRALAM substrate with dielectric constant of 2.55 at 10 GHz. The thickness of the substrate is 30 mil and the thickness of the copper on both sides of the substrate is 1.4 mil. The GaAs MESFETs, NE72084B, are soldered on the proper sites. The top cover of the reactive MESFET is removed in order to receive the incident light from a semiconductor laser for optical-control tuning. Two resistances used for termination are also soldered on the substrate.
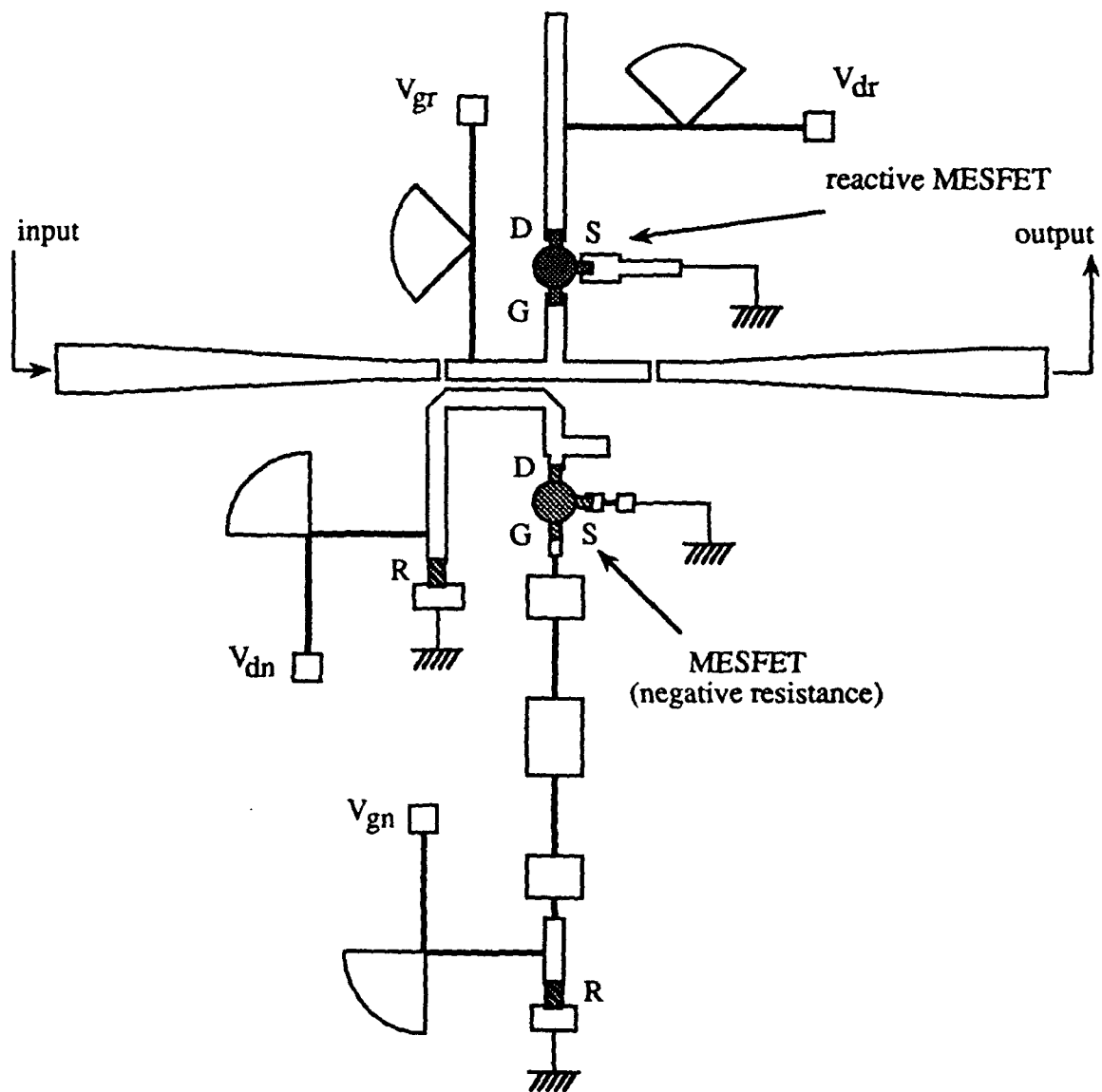
Fig. 3.6   Tunable active bandpass filter using two MESFETs
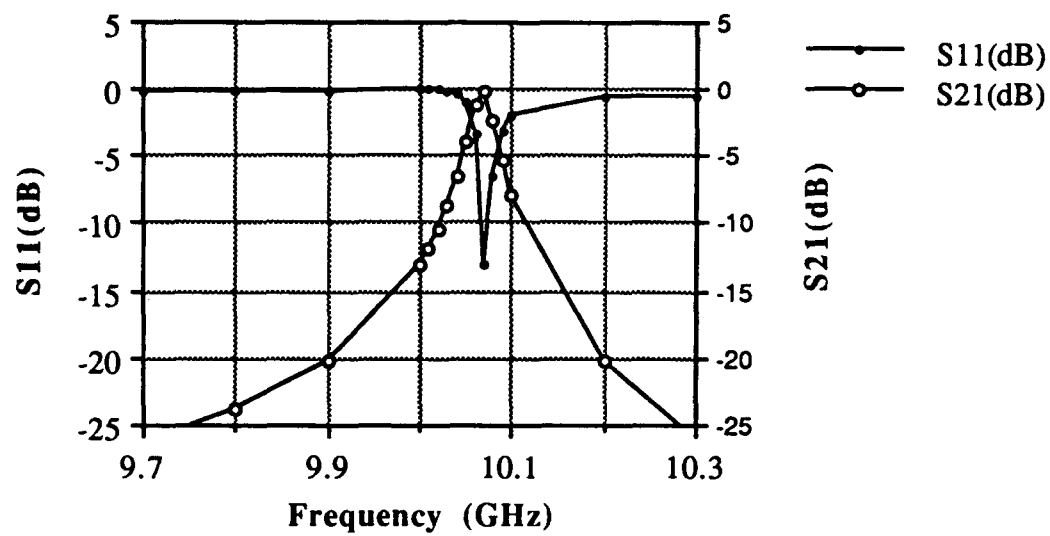
Fig. 3.7 Simulation result of the circuit in Fig. 3.6

3.2 Measurement Result

The S_{11} and S_{21} parameters of this active filter are measured by HP 8510A Vector Network Analyzer. By changing the reactance of the reactive MESFET, center-frequency shift of the passband is observed. If the center-frequency shift is controlled by the bias voltage, it is called *the voltage-control tuning method*. If the center-frequency shift is controlled by the incident light, it is called *the optical-control tuning method*.

3.2.1 Voltage-control Tuning

The voltage-control tuning is made by changing V_{gr}(gate voltage of the reactive MESFET) and keep V_{dr}(drain voltage of the reactive MESFET) unchanged. To prevent making any negative resistance at the input port of the reactance-tuning circuit, V_{dr} is set to zero which is the same as V_{sr}(source voltage of the reactive MESFET). Under such a condition the DC current flowing through the MESFET is zero and the MESFET is not in the active mode.

Fig. 3.8 displays the voltage-tuning performance of this filter. By changing V_{gr} from 0V to -5.43V, the center-frequency of the passband shifts from 9.649 GHz to 9.818 GHz. The tuning range is about 170 MHz. The voltage dependence of the center frequency is shown in Fig. 3.9. As V_{gr} is increased, the center frequency decreases. This can be explained by the MESFET model in Chapter 2. When V_{gr} is increased, the depletion region decreases and both C_{gs} and C_{gd} increase; thus the effective electrical length of the resonant tank increases. Hence, the center frequency of the passband is decreased.

Since the center-frequency of the passband can also be tuned by changing the bias voltages of the MESFET used to generate a negative resistance, which will be discussed in the next chapter, it is possible to tune the center-frequency by both MESFETs in this filter. The voltage-tuning performance using both MESFETs is displayed in Fig. 3.10 and the

19

voltage dependence of the center frequency is listed in Table 3.1. With the aid of both MESFETs, a tuning range of 240 MHz is obtained.
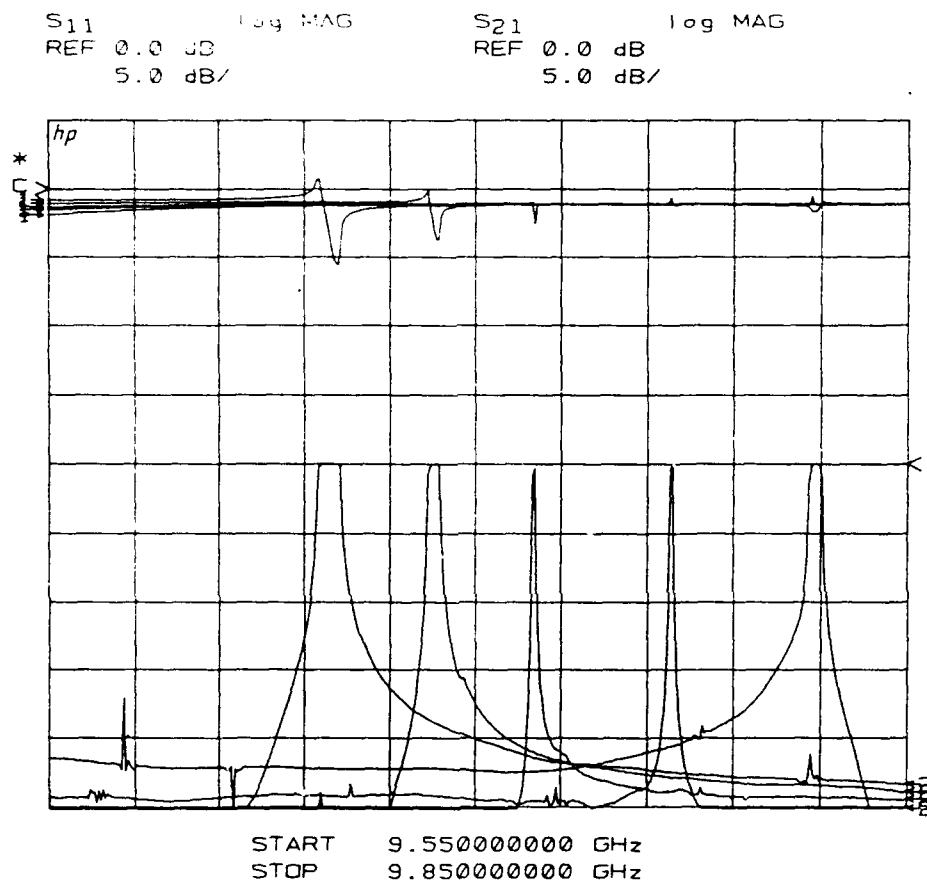
Fig. 3.8   Voltage-control tuning by the reactive MESFET of the filter in Fig. 3.6

Bias condition : $V_{gn} = -0.83V$

$V_{dn} = 1.4V$

$V_{dr} = 0V$

20
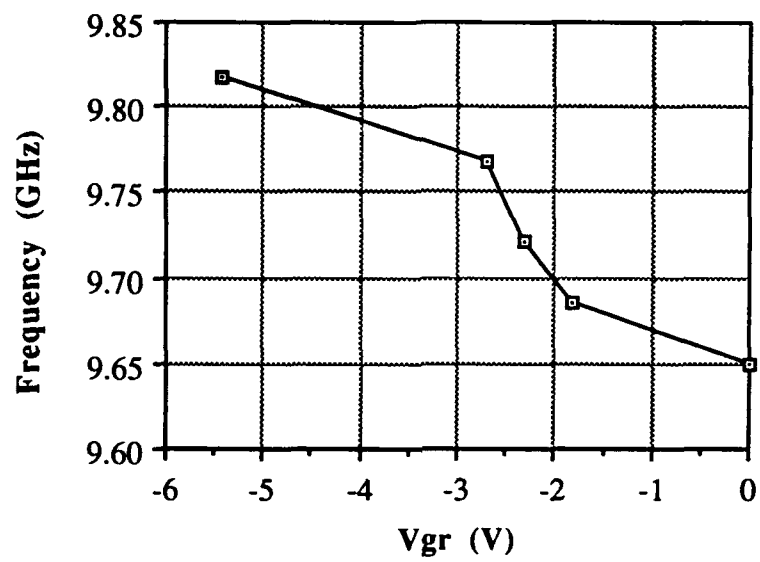
Fig. 3.9 Center-frequency of the passband as a function of V_{gr}

(related to the measurement result in Fig. 3.8)

21

S$_{11}$ log MAG   S$_{21}$ log MAG
REF 0.0 dB   REF 0.0 dB
     5.0 dB/   5.0 dB/

hp

START   9.550000000 GHz
STOP   9.850000000 GHz
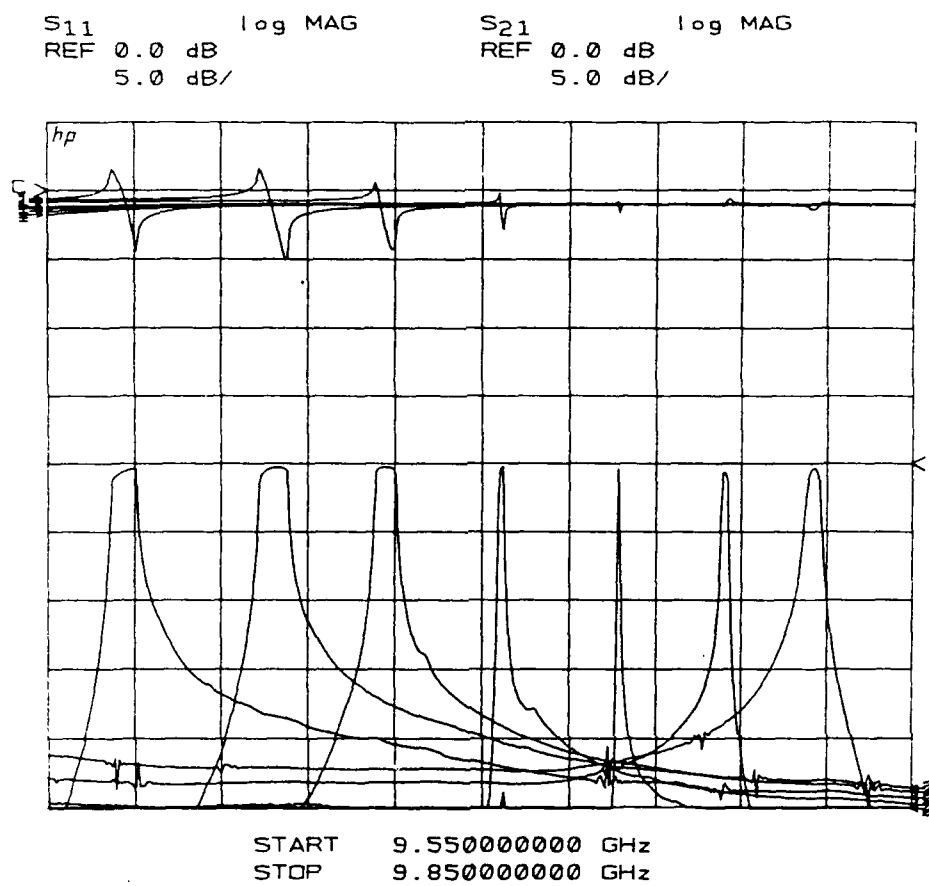
Fig. 3.10   Voltage-control tuning by both MESFETs of the filter in Fig. 3.6

22

Frequency(GHz)	V_{gr} (V)	V_{dn} (V)	V_{gn} (V)
9.816	-5.40	1.42	-0.98
9.785	-2.98	1.42	-0.98
9.748	-2.54	1.60	-0.98
9.708	-2.21	1.60	-0.98
9.667	-0.98	1.57	-0.98
9.630	0	2.20	-1.21
9.577	0	6.00	-1.31

Table 3.1   Center frequency of the passband as a function of bias voltages

(related to the measurement result in Fig. 3.10)

23

3.2.2 Optical-control Tuning

In addition to the voltage-control tuning method, the passband of the filter can be controlled by optical illumination. To receive the illumination from a light source, the top cover of the reactive MESFET is removed. A Sharp® LT021MC0 semiconductor laser diode with wavelength of 788 nm and maximum output power of 15 mW is used as the light source. The laser light is focused on the MESFET chip with a fine-tuning of the focal point in the region between gate and source and/or between gate and drain. The depletion region under the gate is influenced by the laser light and thus the capacitance C_{gs} is changed. The optical-control tuning performance is measured and shown in Fig. 3.11. The center frequency as a function of laser output power is shown in Fig. 3.12. When the light intensity increases, the center frequency decreases because the carriers generated inside the depletion region reduce C_{gs} and C_{gd}, which in turn increases the effective electrical length of the resonant tank. When the output power of the semiconductor laser diode is changed from 0 mW to 15 mW, the tuning range is 50 MHz.
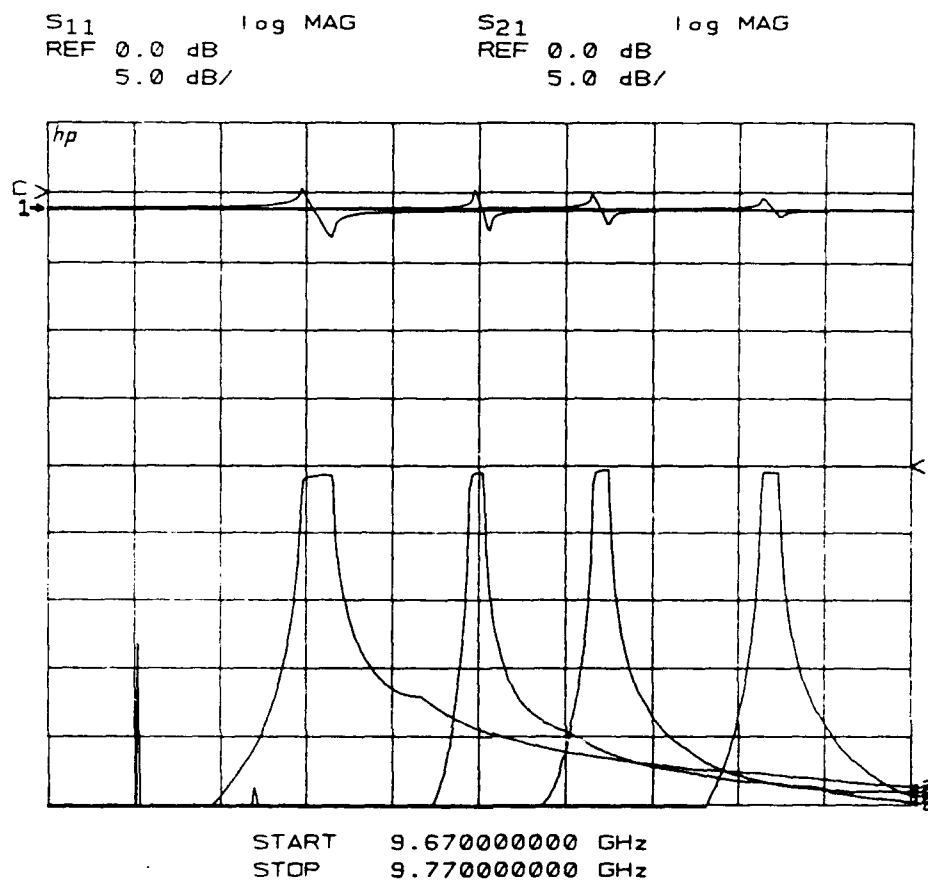
Fig. 3.11 Optical-control tuning of the filter in Fig. 3.6

Bias condition : V_{gn} = -0.83V

V_{dn} = 1.4V

V_{dr} = 0V

V_{gr} = -2.53V
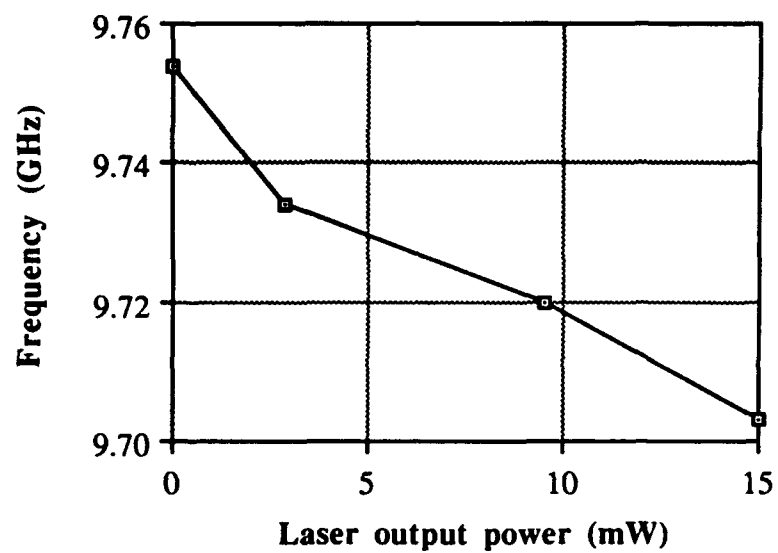
Fig. 3.12   Center frequency of the passband as a function of laser output

power

(related to the measurement result of Fig. 3.11)

Chapter 4
Tunable Active Bandpass Filter Using One MESFET

In Chapter 3, a tunable active bandpass filter using two MESFETs is discussed. These two MESFETs in the filter have different functions. One is used in active mode to generate a negative resistance while the other is used in reactive mode to provide a variable reactance. However, from the discussions in Chapter 2, we found that the MESFET also has the characteristic of variable reactance in the active mode. Therefore, a new idea to replace these two MESFETs with only one MESFET is investigated. The MESFET can function as both negative resistance and three-terminal varactor at the same time. It is possible to make a tunable active bandpass filter with only one MESFET. This chapter presents such a tunable active bandpass filter.

4.1 Circuit Design, Simulation and Fabrication

The most important consideration here is the negative resistance value from the MESFET. In order to keep the S_{21} value of the center frequency at 0 dB through the tuning range, the negative resistance needs to be controlled to a constant value. When the reactance is changed by the bias voltage, the negative resistance changes in general. However, the negative resistance should not change much when the drain voltage is larger than the saturation voltage, because I_{ds} saturates beyond this point. With this feature, it is possible to tune the center frequency of passband by changing V_d without disturbing the negative resistance significantly.

At first, the circuit is designed from the circuit pattern in Fig. 3.6 by removing the reactance-tuning circuit away. In such a case the voltage-control tuning range is found to be less than 50 MHz. In order to change the effective electrical length of resonant tank more, the gap width between the coupled lines is decreased so that the coupling coefficient is

27

increased. However, the effect of the negative resistance is increased in this case. Hence, V_g needs to be smaller to reduced the negative resistance so that the passband insertion loss does not change. Referring to Fig. 2.7, it is observed that the slope of the C-V curve which corresponds to the variation range of capacitance becomes smaller when Vg is smaller. Therefore, there exists an optimum point of Vg and gap width for maximum tuning range.

This compromise is approached by reducing the gap width between coupled lines from 18 mil in Fig. 3.2 to 8 mil in Fig. 4.1, which is corresponding to a gate voltage of -1.6V. The new circuit is almost the same as the circuit in Fig. 3.2 except a minor modification. Details of this circuit is shown in Appendix B. The simulation result of the filter performance at a fixed bias condition is shown in Fig. 4.2.

input

output

D

G   S

V_d

R

MESFET

V_g

R

D: drain
G: gate
S: source
R: termination resistance
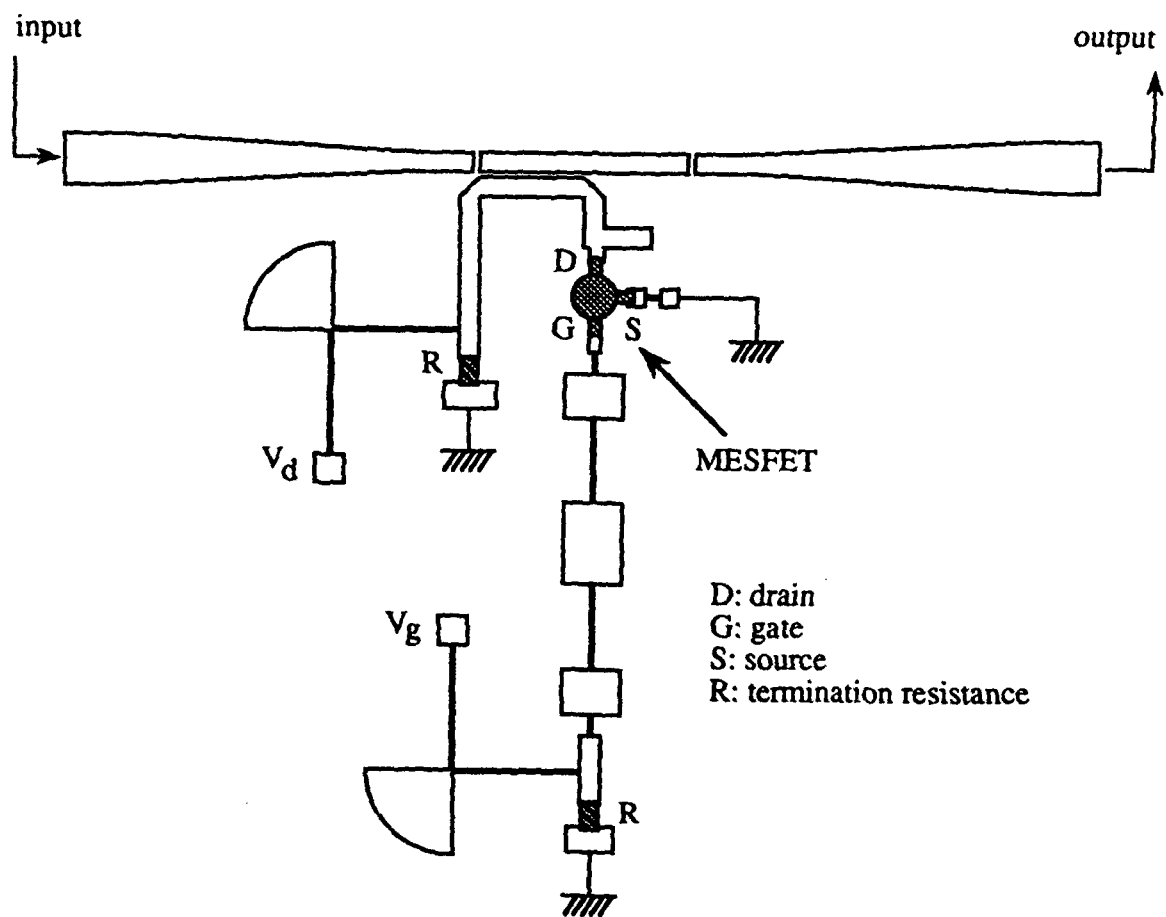
Fig. 4.1   Tunable active filter using one MESFET
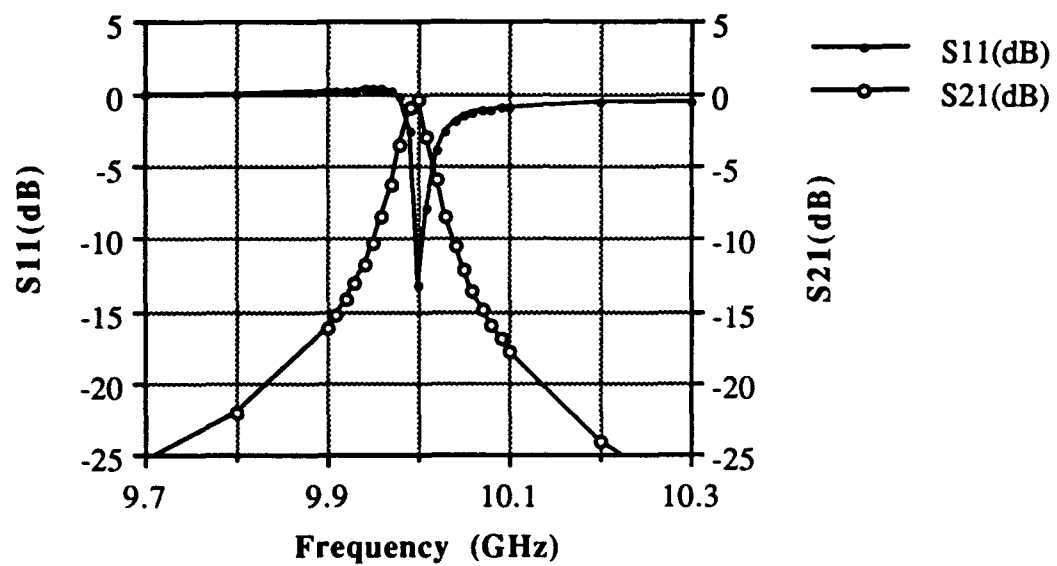
Fig. 4.2   Simulation result of the circuit in Fig.4.1

4.2 Measurement Result

4.2.1 Voltage-control Tuning

Three methods of voltage-control tuning are discussed here. The first method is to change V_d while V_g is unchanged, as shown in Fig. 4.3. The tuning range is 120 MHz. The second method is to change V_g while V_d is unchanged, as shown in Fig. 4.4. The tuning range for this method is 90 MHz. The third method is to change both V_d and V_g, as shown in Fig. 4.5. The tuning range obtained is 150 MHz. The voltage dependences of the center frequency for these three methods are shown in Fig. 4.6, Fig. 4.7 and Table 4.1, respectively.

The measurement result can be explained by the reactive MESFET model in Chapter 2. The tuning response of Fig. 4.6 can be explained by referring to Fig. 2.8. With V_g biased at -1.6V, the capacitance between the drain terminal and the source terminal increases as V_d is increased. Then, the effective electrical length of resonant tank is increased and the center frequency of passband is decreased. The tuning response of Fig. 4.7, however, can not be explained by Fig. 2.8 because V_g is larger than the pinch-off voltage and the channel is open. It should be explained by Fig. 2.3(a) because C_{gs} is dominant now. Referring to Fig. 2.3(a), C_{gs} increases as V_g is increased. The effective electrical length of resonant tank is hence increased and the center frequency of passband is decreased.

Comparing the V_d-tuning and the V_g-tuning methods, it is found that the former method is superior to the other since a wider tuning range of 120 MHz is obtained. Moreover, a tuning range of 150 MHz can be achieved with the aid of V_g.

S₁₁ log MAG   S₂₁ log MAG
REF 0.0 dB   REF 0.0 dB
5.0 dB/   5.0 dB/
-3.6953 dB   1 -2.912 dB
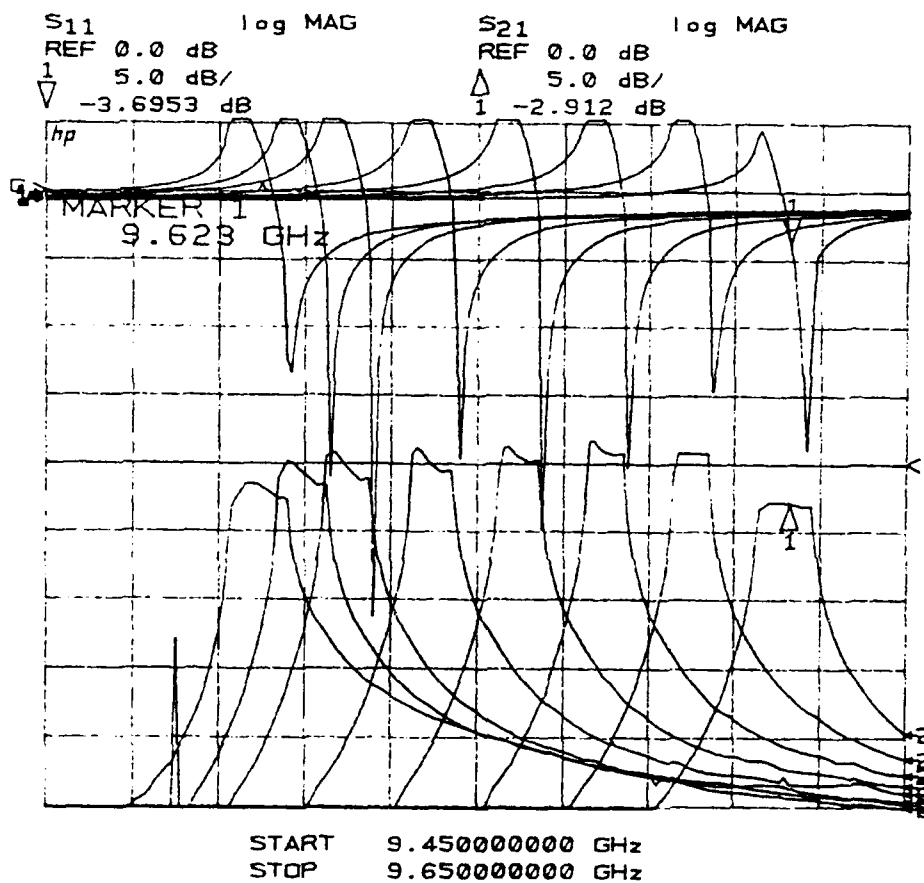
Fig. 4.3 V_d-tuning of the filter in Fig. 4.1 ($V_g = -1.6V$)

S11   log MAG   S21   log MAG
REF 0.0 dB   REF 0.0 dB
1   5.0 dB/   △   5.0 dB/
▽ 1.5139 dB   1 -1.0023 dB

hp

MARKER 1
9.618 GHz

START   9.450000000 GHz
STOP   9.650000000 GHz
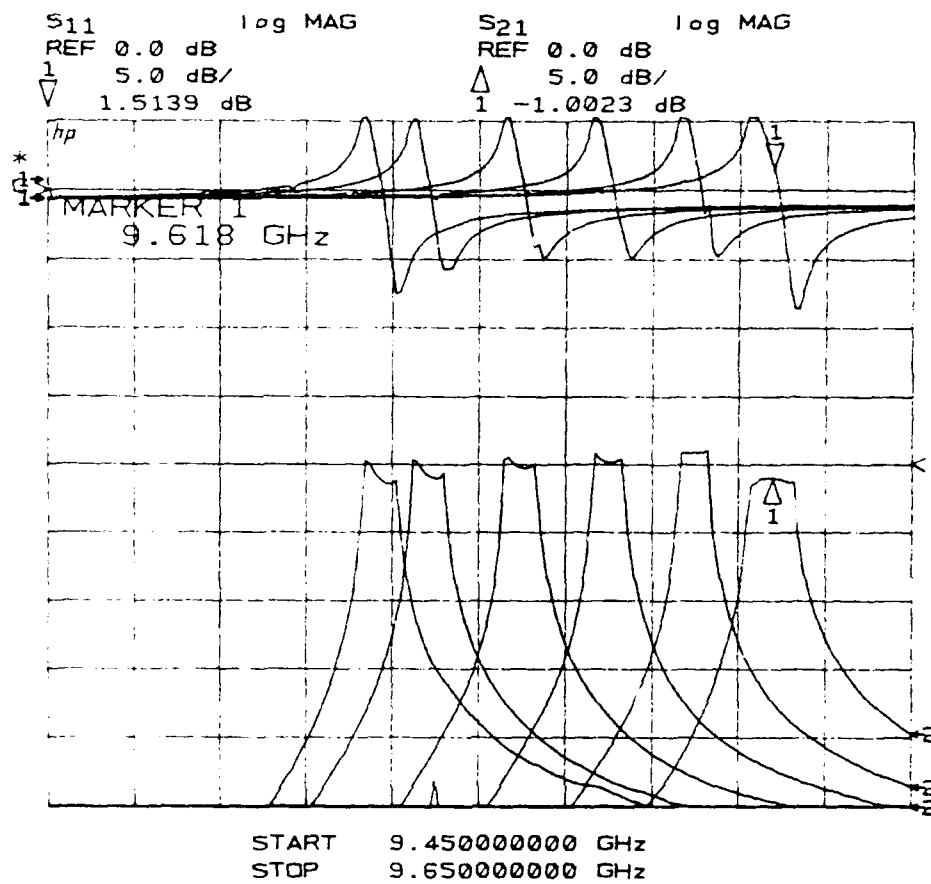
Fig. 4.4   V$_g$-tuning of the filter in Fig. 4.1 (V$_d$ = 3V)

33
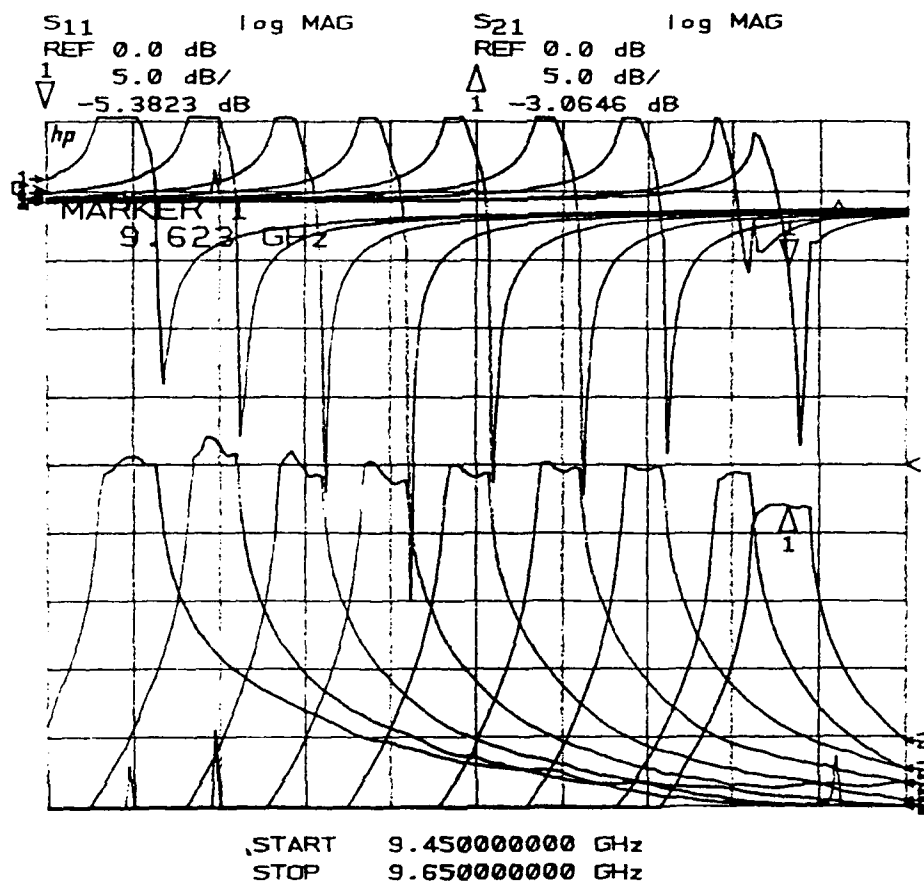
Fig. 4.5 Voltage-tuning of the filter in Fig. 4.1 (Using both V_d and V_g)

34
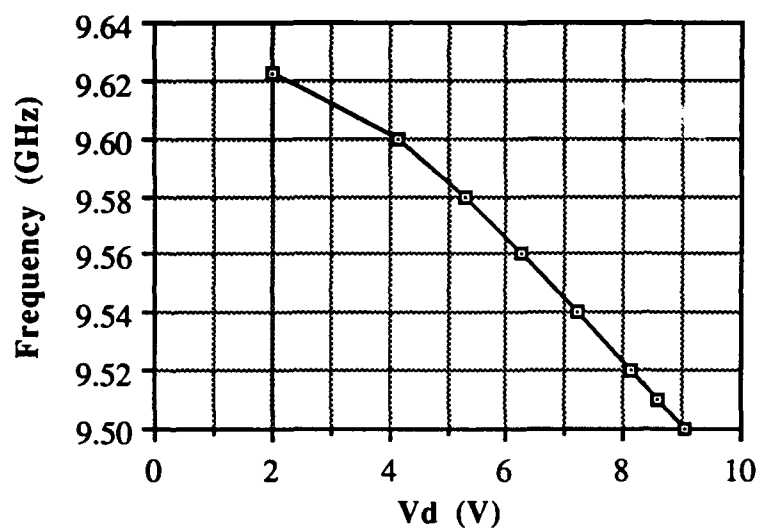
Fig. 4.6 Center frequency of the passband as a function of V_d

(related to the measurement result in Fig. 4.3)
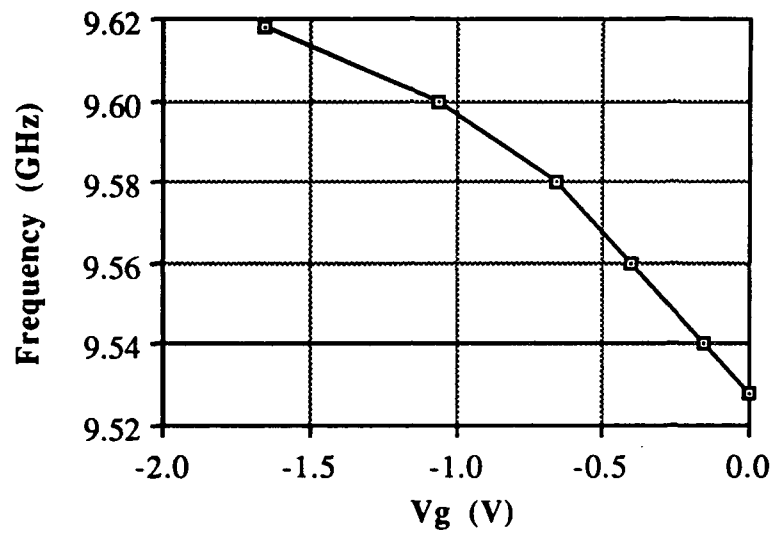
Fig. 4.7   Center frequency of the passband as a function of V_g

(related to the measurement result in Fig. 4.4)

Frequency (GHz)	V_d (V)	V_g (V)
9.623	1.85	-1.38
9.610	2.27	-1.38
9.590	4.59	-1.67
9.570	5.68	-1.67
9.550	6.66	-1.64
9.530	7.56	-1.64
9.510	8.21	-1.55
9.490	5.22	0
9.470	5.48	0

Table 4.1   Center frequency of the passband as a function of bias voltages

(related to the measurement result in Fig. 4.5)

4.2.2 Optical-control Tuning

The optical-control tuning range is less than 10 MHz, which is much smaller than the optical-tuning range of the filter using two MESFETs. The reason is found from the bias voltage V_g. In order to have the widest optical-control tuning range, the gate voltage of the MESFET receiving the incident light must be biased at a specific voltage which corresponds to the widest capacitance tuning range(Fig. 2.3(a))[3]. This voltage is usually below -2V. For instance, the widest optical-control tuning range of 50 MHz for the filter using two MESFETs is obtained by keeping the gate voltage of the reactive MESFET at -2.53V. However, for the filter with only one MESFET, the latter cannot be biased at such a voltage because a negative resistance requires V_g to be at a much larger value. For example, V_g is biased at -1.6V in V_d-tuning and is varied from -1.6V to 0V in V_g-tuning. In this range the optical-control tuning range is very small.

Although the optical-control tuning is not practical for the filter with one MESFET, the achievement of using one MESFET to replace two MESFETs in the tunable active bandpass filter is still significant. The advantage brought in by this improvement is that the fabrication of this circuit is simplified and the operation of this circuit is simpler because only one MESFET is needed.

4.2.3 Temperature Effect

The stability of the filter with temperature variation is studied. The room temperature is changed slowly from 70°F to 80°F in two hours. The center frequency of passband shifts by 2 MHz. The MESFET is then heated by a temperature-controllable soldering iron setting at 250°F. The soldering iron head is put on the top cover of the MESFET until thermal equilibrium is reached, i.e., the center frequency of the passband does not change further. In this case, the center frequency of passband shifts 10 MHz more. The measurement result is shown in Fig. 4.8 and the temperature dependence is

drawn in Fig. 4.9. According to the measurement result, this filter is not sensitive to the temperature variation.
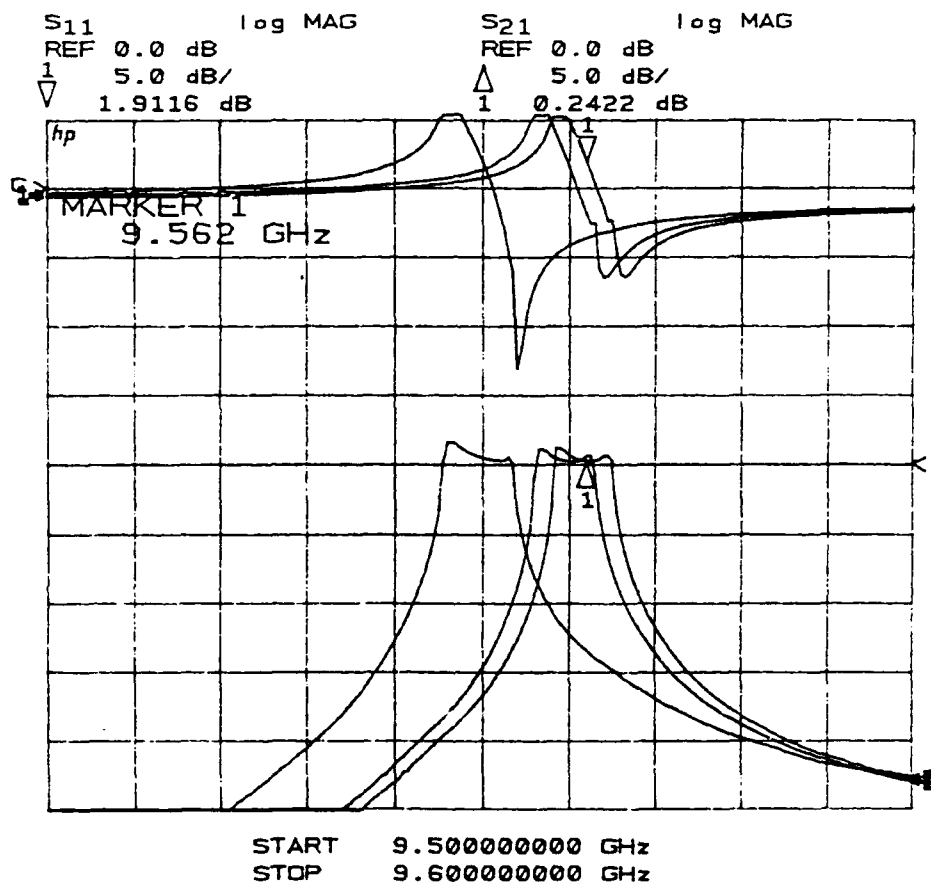
Fig. 4.8 Temperature effect of the filter in Fig. 4.1
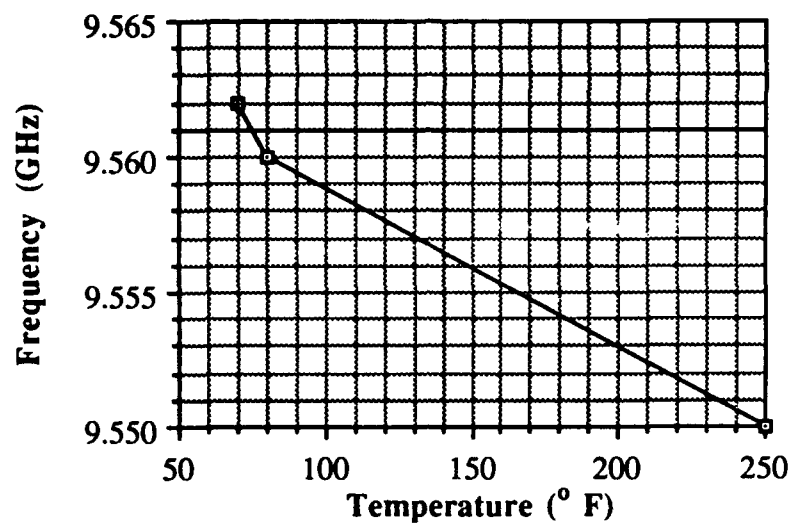
Fig. 4.9 Temperature dependence of the center frequency

(related to the measurement result in Fig. 4.8)

40

Chapter 5
Conclusion

Based on the concept of three-terminal MESFET varactor, two types of tunable active bandpass filter are made. The first circuit uses two MESFETs of which one is used as a MESFET varactor and the other is used to generate a negative resistance compensating the loss of the tank circuit. The second circuit uses only one MESFET which has both functions of the two MESFETs in the first circuit. Both circuits use the MESFET as a three-terminal varactor. This is different from using MESFET as a two-terminal varactor[2][3][4].

For the first circuit using two MESFETs, three kinds of operations are observed. The voltage-control tuning using the gate voltage of the reactive MESFET gives a tuning range of 170 MHz. The voltage-control tuning using both the reactive MESFET and the negative resistance MESFET gives a wider tuning range of 240 MHz. The optical-control tuning, with a semiconductor laser as the light source, gives a tuning range of 50 MHz.

For the second circuit using one MESFET, three kinds of operations are observed. The voltage-control tuning using the gate voltage of the MESFET gives a tuning range of 90 MHz. The voltage-control tuning using the drain voltage of the MESFET gives a tuning range of 120 MHz, which is better than the tuning controlled by the gate voltage. If both the drain voltage and the gate voltage are used, a wider tuning range of 150 MHz is obtained. The optical-control tuning is not practical for this filter because the tuning range is less than 10 MHz. The reason is that the gate of the MESFET needs to be biased at a much higher voltage than the optimum voltage for the optical-control tuning to generate a negative resistance which compensates the loss of the circuit. The temperature effect of this circuit is

41

also studied and the result shows that this filter is not sensitive to the temperature variation.

Compared to the previous results using the MESFET as a two-terminal varactor, the most significant advantage of using the MESFET as a three-terminal varactor is to let the MESFET have two different functions at the same time. The MESFET is used as an active device which amplifies signal. With the analysis of the relationship between the internal capacitances and the bias condition, the MESFET is found to have a reactance-tuning capability in the active mode if it is biased properly. This finding demonstrates the potential of using both real and imaginary parts of the equivalent impedances of the active devices.

Appendix A
Circuit File of The Tunable Active Bandpass Filter Using Two MESFETs

DIM   ! Default units used in this circuit file

    FREQ   GHZ   ! GHz

    RES   OH   ! Ohm

    IND   NH   ! nH

    CAP   PF   ! pF

    LNG   MIL   ! mil

    ANG   DEG   ! Degree

VAR

    W0=33.6   ! width of the line for 82Ω

    WBIAS=5   ! width of the bias line

    G=15   ! gap width between tank and I/O lines

    GCOUP=18   ! gap width between coupled lines

    COUP=187.3   ! length of the coupled line in tank

    UNCOUP=153.7   ! length of the uncoupled line in tank

    LBIAS=217   ! half-wavelength in bias line

CKT

    MSUB ER=2.55 H=30 T=1.4 RHO=0.8 RGH=0   ! data of the substrate

    TAND TAND=0.002   ! loss tangent of the substrate

!

    MLIN 1 2 W^WBIAS L^LBIAS   ! half wavelength

    MTEE 2 3 4 W1^WBIAS W2^WBIAS W3^WBIAS !

    MLIN 3 5 W^WBIAS L^LBIAS   ! half wavelength

    MRSTUB 4 WI^WBIAS L=150 ANG=90   ! short

    MSTEP 5 6 W1^WBIAS W2=40   !

    MLOC 6 W=40 L=40   !

    DEF1P 1 BIAS   ! bias CKT

!

    MLIN 3 4 W=5 L=36.61   ! inductance

    MSTEP 4 5 W1=5 W2=100   !

    MLIN 5 6 W=100 L=77.37   ! capacitance

```
MSTEP 6 7 W1=100 W2=5                    !
MLIN 7 8 W=5 L=148.26                     ! inductance
MSTEP 8 9 W1=5 W2=100                     !
MLIN 9 10 W=100 L=70.43                   ! capacitance
DEF2P 3 10 HALFF                          !
HALFF 1 2                                 !
HALFF 3 2                                 !
DEF2P 1 3 LPF                             ! low pass filter CKT
!

S2PA 11 12 13 NE72084B                    ! S-parameter of MESFET
MLIN 11 1 W=20 L=35                       ! line from gate to LPF
MSTEP 1 51 W1=20 W2=5                     !
LPF 51 2                                  !
MSTEP 2 52 W1=50 W2^W0                    !
MLIN 52 53 W^W0 L=120                     ! line from LPF to termination
SRL 53 0 R=82 L=0.15                      ! termination resistance
MLIN 13 14 W=30 L=30                      !
MSTEP 14 15 W1=30 W2=5                    !
MLIN 15 21 W=5 L=27                       ! line from source to ground
MSTEP 21 22 W1=5 W2=30                    !
MLIN 22 23 W=30 L=15                      !
VIA 23 0 D1=10 D2=10 H=30 T=1             ! via hole connected to ground plane
MLOC 23 W=30 L=15                         !
MLIN 12 6 W=25 L=25                       ! line from drain to output
DEF1P 6 NR                               ! negative resistance CKT
!

MLIN 1 2 W=87.5 L=100                     ! 50Ω line
MTAPER 2 3 W1=87.5 W2^W0 L=518            ! transition from 50Ω to 82Ω
MLIN 3 4 W^W0 L=100                       ! 82Ω line
DEF2P 1 4 FEED                            ! feed CKT
!

MLIN 1 5 W=33.6 L=126                     ! line from gate to output
S2PB 5 6 7 NE72084A                       ! S-parameter of MESFET
MLIN 7 8 W=50 L=70                        !
MSTEP 8 9 W1=50 W2=25                     !
```

44

```
    MLSC 9 W=25 L=110                             ! line from source to ground
    MLIN 6 10 W=33.6 L=205                        !
    MTEE 11 10 12 W1=33.6 W2=33.6 W3=5            !
    MLOC 11 W=33.6 L=205                          ! line from drain to open
    BIAS 12                                       !
    DEF1P 1 REACT                                 ! reactance-tuning CKT
!
    TAND TAND=0.038                               ! emulation of the radiation loss
    MCLIN 4 5 6 7  W^W0 S^GCOUP L^COUP            ! coupled line in tank
    MTEE2 7 8 9 W1^W0 W2^W0 W3^W0                 !
    MLIN 8 13 W^W0 L^UNCOUP                       ! uncoupled line in tank
    TAND TAND=.002                                ! back to the normal loss tangent
    REACT 9                                       !
    MBEND3 5 11 W^W0                              !
    MBEND3 6 21 W^W0                              !
    MLIN 11 12 W^W0 L=271.9                       ! line from coupled line to termination
    MLIN 21 22 W^W0 L=53.4                        ! line from coupled line to NR
    MTEE2 23 22 24 W1^W0 W2^W0 W3^W0              !
    MLOC 24 W^W0 L=77.6                           ! matching stub
    MSTEP 23 25 W1^W0 W2=25                       !
    NR 25                                         !
    SRL 12 0 R=82 L=0.15                          ! termination resistance
    DEF2P 4 13 TANK                               ! resonant tank CKT
!
    FEED 1 2                                      ! input
    MGAP 2 3 W^W0 S^G                             !
    TANK 3 4                                      ! resonant tank
    MGAP 4 7 W^W0 S^G                             !
    FEED 8 7                                      ! output
    DEF2P 1 8 FILTER                              ! filter CKT
FREQ
    SWEEP 9.7 10.0 0.1
    SWEEP 10.0 10.1 0.01
    SWEEP 10.1 10.3 0.1
OUT
```

```
    FILTER DB[S11] GR1
    FILTER DB[S21] GR1
GRID
    RANGE 9.7 10.3 0.1
    GR1 -25 5 5
```

Appendix B
Circuit File of The Tunable Active Bandpass Filter Using One MESFET

DIM   ! Default units used in this circuit file

    FREQ   GHZ   ! GHz

    RES   OH   ! Ohm

    IND   NH   ! nH

    CAP   PF   ! pF

    LNG   MIL   ! mil

    ANG   DEG   ! Degree

VAR

    W0=33.6   ! width of the line for 82Ω

    WBIAS=5   ! width of the bias line

    G=15   ! gap width between tank and I/O lines

    GCOUP=8   ! gap width between coupled lines

    COUP=181   ! length of the coupled line in tank

    UNCOUP=181   ! length of the uncoupled line in tank

    LBIAS=217   ! half-wavelength in bias line

CKT

    MSUB ER=2.55 H=30 T=1.4 RHO=0.8 RGH=0   ! data of the substrate

    TAND TAND=0.002   ! loss tangent of the substrate

!

    MLIN 1 2 W^WBIAS L^LBIAS   ! half wavelength

    MTEE 2 3 4 W1^WBIAS W2^WBIAS W3^WBIAS   !

    MLIN 3 5 W^WBIAS L^LBIAS   ! half wavelength

    MRSTUB 4 W1^WBIAS L=150 ANG=90   ! short

    MSTEP 5 6 W1^WBIAS W2=40   !

    MLOC 6 W=40 L=40   !

    DEF1P 1 BIAS   ! bias CKT

!

    MLIN 3 4 W=5 L=36.61   ! inductance

    MSTEP 4 5 W1=5 W2=100   !

    MLIN 5 6 W=100 L=77.37   ! capacitance

```
MSTEP 6 7 W1=100 W2=5                    !
MLIN 7 8 W=5 L=148.26                    ! inductance
MSTEP 8 9 W1=5 W2=100                    !
MLIN 9 10 W=100 L=70.43                  ! capacitance
DEF2P 3 10 HALFF                         !
HALFF 1 2                                !
HALFF 3 2                                !
DEF2P 1 3 LPF                            ! low pass filter CKT
!
S2PA 11 12 13 NE72084B                   ! S-parameter of MESFET
MLIN 11 1 W=20 L=35                      ! line from gate to LPF
MSTEP 1 51 W1=20 W2=5                    !
LPF 51 2                                 !
MSTEP 2 52 W1=50 W2^W0                   !
MLIN 52 53 W^W0 L=120                    ! line from LPF to termination
SRL 53 0 R=82 L=0.15                     ! termination resistance
MLIN 13 14 W=30 L=30                     !
MSTEP 14 15 W1=30 W2=5                   !
MLIN 15 21 W=5 L=27                      ! line from source to ground
MSTEP 21 22 W1=5 W2=30                   !
MLIN 22 23 W=30 L=15                     !
VIA 23 0 D1=10 D2=10 H=30 T=1            ! via hole connected to ground plane
MLOC 23 W=30 L=15                        !
MLIN 12 6 W=25 L=25                      ! line from drain to output
DEF1P 6 NR                               ! negative resistance CKT
!
MLIN 1 2 W=87.5 L=100                    ! 50Ω line
MTAPER 2 3 W1=87.5 W2^W0 L=518           ! transition from 50Ω to 82Ω
MLIN 3 4 W^W0 L=100                      ! 82Ω line
DEF2P 1 4 FEED                           ! feed CKT
!
TAND TAND=0.038                          ! emulation of the radiation loss
MCLIN 4 5 6 7  W^W0 S^GCOUP L^COUP       ! coupled line in tank
MLIN 7 13 W^W0 L^UNCOUP                  ! uncoupled line in tank
TAND TAND=.002                           ! back to the normal loss tangent
```

```
    MBEND3 5 11 W^W0                          !
    MBEND3 6 21 W^W0                          !
    MLIN 11 12 W^W0 L=269                     ! line from coupled line to termination
    MLIN 21 22 W^W0 L=54.6                    ! line from coupled line to NR
    MTEE2 23 22 24 W1^W0 W2^W0 W3^W0          !
    MLOC 24 W^W0 L=76.9                       ! matching stub
    MSTEP 23 25 W1^W0 W2=25                   !
    NR 25                                     !
    SRL 12 0 R=82 L=0.15                      ! termination resistance
    DEF2P 4 13 TANK                           ! resonant tank CKT
!
    FEED 1 2                                  ! input
    MGAP 2 3 W^W0 S^G                         !
    TANK 3 4                                  ! resonant tank
    MGAP 4 7 W^W0 S^G                         !
    FEED 8 7                                  ! output
    DEF2P 1 8 FILTER                          ! filter CKT
FREQ
    SWEEP 9.7 9.9 0.1
    SWEEP 9.9 10.1 0.01
    SWEEP 10.1 10.3 0.1
OUT
    FILTER DB[S11] GR1
    FILTER DB[S21] GR1
GRID
    RANGE 9.7 10.3 0.1
    GR1 -25 5 5
```

Bibliography

[1] C.-Y. Chang and T. Itoh, "Microwave active filters based on coupled negative resistance method," *IEEE Trans. Microwave Theory Tech.*, vol. MTT-38, pp. 1879-1884, December 1991.

[2] Y. Yamamoto, K.-I. Kawasaki, and T. Itoh, "A MESFET-controlled X-band active band-pass filter," *IEEE Microwave and Guided Wave Letters*, vol. 1, pp. 110-111, May 1991.

[3] Y. Yamamoto, K.-I. Kawasaki, and T. Itoh, "Optical control of microwave active bandpass filter using MESFETs," *IEEE MTT-S Digest 1991*, vol. 2, pp. 655-658.

[4] Y. Yamamoto, J. Lin, and T. Itoh, "Laser tuning of a planar active bandpass filter using MESFETs," *Conference Proceedings of 21th European Microwave Conf.*, Sept. 1991.

[5] M. Shur, "Physics of semiconductor devices," Prentice Hall, New Jersey, 1990, pp. 416-417.

[6] W. R. Curtice, "A MESFET model for use in the design of GaAs integrated circuits," *IEEE Trans. Microwave Theory Tech.*, vol. MTT-28, pp. 448-456, May 1980.

[7] T. Takada, K. Yokoyama, M. Ida, and T. Sudo, "A MESFET variable-capacitance model for GaAs Integrated Circuit Simulation," *IEEE Trans. Microwave Theory Tech.*, vol. MTT-30, pp. 719-723, December 1982.

[8] H. A. Willing, C. Rauscher, and P. deSantis, "A technique for predicting large -signal performance of a GaAs MESFET," *IEEE Trans. Microwave Theory Tech.*, vol. MTT-26, pp. 1017-1023, December 1978.

[9] R. W. H. Engelmann and C. A. Liechti, "Gunn domain formation in the saturated region of the GaAs MESFETs," *IEEE Int. Electron Device Conf. Digest*, 1976, pp. 351-354.